Stephan Rauschenbach, Klaus Kern

EXPLORING COMPLEX MOLECULAR FUNCTIONALITY AT SURFACES

INTRODUCTION

One of the most powerful paradigms of nanoscale science[1] is that the properties of a nanometer sized object can be affected by the presence or absence of even a single atom. Henceforth the current challenge of nanotechnology is the understanding and controlling of the vast complexity which arises when nanoscale objects interact with the environment. To master this problem, novel approaches are needed, capable of comprehensive characterization of the physical and chemical properties of nanoscale systems with atomic resolution. Required is nothing less than the precise knowledge of the atomic structure, which means atomic positions just as well as chemical information about each atom of a nanoscale object, like a molecule.

Scanning probe microscopy (SPM)[2, 3] plays a central role in nanotechnology research because it makes the direct observation of atoms and molecules possible and even allows for their individual manipulation.[4, 5] Recording the mutual interaction of an atomically sharp tip with a surface, scanning probe microscopes map the surface, resolving sub-nanometer features or even single atoms (Fig. 1a,b).[6, 7] The recorded quantity is the tunnel current in a scanning tunneling microscope (STM), or the frequency shift of an oscillating cantilever due to the exerted forces in an atomic force microscope (AFM). The tunneling current in STM is related to the integrated local density of electronic states (LDOS) in the energy window between the applied bias and the Fermi energy. In AFM, the short-range forces from the attractive chemical bonding and the repulsive Pauli interaction decay at atomic length scale and are the origin of the atomic resolution topography, modulated by long-range Van-der-Waals and electrostatic forces.[8, 9]

In addition to imaging surfaces, SPM allows accessing the tip-surface interaction spectroscopically.[10] With the tip placed still over a specific location, a spectrum is recorded as a function of parameters like bias voltage, tip-surface distance, or oscillation amplitude depending on the configuration of the setup, i.e. STM, AFM, etc. (Fig. 1c). These measurements reveal the local electronic structure[10] or inelastic excitations like bond vibrations[11], magnetic excitations (STM)[12, 13], or interaction potentials (AFM)[5]. Combining spectroscopic and spatial information yields maps of physical properties over a part of the surface with atomic precision, as for instance density of states, chemical potential, work function[14, 15], surface charge[16], or orbital shape.[17]

Reaching the best performance in SPM relies strongly on the quality of the samples. Usually only atomically flat crystal surfaces in ultrahigh vacuum (UHV) are suitable. On them, well-defined adsorbate films are prepared by vacuum evaporation of atoms or molecules. On such atomically defined samples individual molecules can be investigated with spatial precision at the atomic level. The direct extraction of chemical information from SPM data, however, is almost impossible, due to the fact that the electronic states of neighboring atoms strongly interact.

Mass spectrometry (MS), in contrast, is the most powerful method to reveal the chemical composition of molecules. Mass spectrometers easily resolve a mass difference much lower than a single proton mass. In other words, MS reaches atomic precision in mass just like SPM is atomically precise in space. It entered the field of molecular nanoscience with the advent of soft ionization methods like electrospray ionization (ESI) and matrix assisted laser desorption ionization (MALDI), which made large, nonvolatile, organic or biological molecules accessible as intact, molecular, gas-phase ions.[18-20]

Despite the ability to measure mass with extreme precision even in very large molecules, MS does not offer a direct route to molecular structure. Due to the importance of structural information mass spectrometers are often combined with structure sensitive methods, typically targeting the gas phase ion. Nearly every mass spectrometry application today includes either fragmentation[21] (collision/surface induced dissociation; CID, SID), hydrogen-deuterium exchange (HDX)[22], ion mobility spectrometry (IMS)[23], or covalent cross linking[24]. By these approaches molecular structure is in principle also investigated by atom sized probes, however the information provided can be very rough, incomplete, or convoluted. IMS, for instance, measures the collision cross section by which it is possible to distinguish differences at the atomic scale. However the complex

Dr. Stephan Rauschenbach
Max-Planck-Institute for Solid State Research
Heisenbergstr. 1, D-70569 Stuttgart, Germany
E-Mail: s.rauschenbach@fkf.mpg.de
http://www.fkf.mpg.de/kern/

Prof. Dr. Klaus Kern
Max-Planck-Institute for Solid State Research
Heisenbergstr. 1, D-70569 Stuttgart, Germany and
École Polytechnique Fédérale de Lausanne
CH-1015 Lausanne, Switzerland
E-Mail: k.kern@fkf.mpg.de
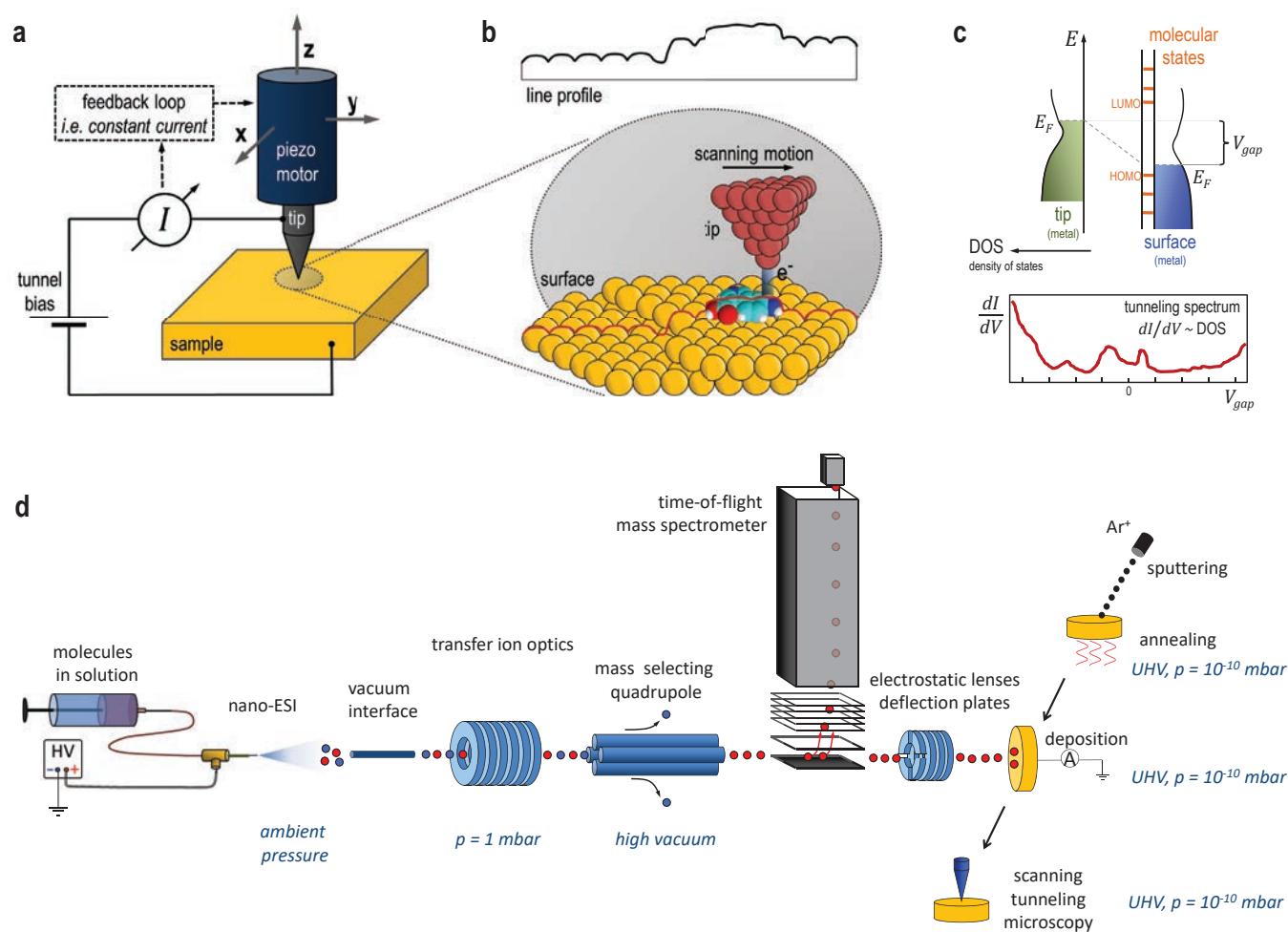
Fig. 1: Scanning Probe Microscopy and Electrospray Ion Beam Deposition. (a) Schematic of the principle of scanning tunneling microscopy. (b) Topographic images are assembled from many line profiles. (c) Scheme of tunneling spectroscopy accessing the local density of states. (d) Scheme of an ES-IBD/SPM experiment. The ion beam is generated by ESI at ambient pressure (left) and transferred to UHV via a differentially pumped vacuum system (pressures given). The SPM sample is prepared under UHV conditions and is transferred in-situ into a deposition stage and finally to the SPM analysis.

information of the three-dimensional (3d) molecular structure is thereby reduced to just one number, the collision cross section. Nevertheless, through systematic measurements combined with modeling, meaningful structural information can be extracted.[25, 26]

Comparing strength and weaknesses of mass spectrometry and scanning probe microscopy shows quite complementary methods. With soft ionization sources even the largest biological molecules are available to MS for chemical characterization, whereas structural information is difficult to access. Through SPM, molecular structure can be imaged at atomic/sub-nanometer resolution, whereas the chemical composition remains obscured. In addition, the SPM imaging of large, complex molecules, in particular biological molecules, is restricted by the condition of evaporability, needed to prepare chemically pure adsorbates on atomically defined metal surfaces in UHV.

Here, preparative mass spectrometry (pMS) presents itself as the perfect link between mass spectrometry and surface science experiments like SPM by providing the well-defined, molecular ion beam of high chemical purity needed for UHV-grade sample preparation.[27]

Preparative mass spectrometry is defined as the mass-selected deposition of (molecular) ions onto a surface. This definition also includes the terms ion soft/reactive landing or ion beam deposition (IBD), which are used synonymously. In principle, soft ionization sources can generate ion beams of large, non-volatile molecules for any vacuum method, including vacuum deposition. An ion beam can simply be directed onto a surface in vacuum where the material is collected, instead of being detected generating the counts of a mass spectrum. Mass filters, as they are employed in a mass spectrometer, can just as well be set to transmit only one ion species for deposition, preferable if they permit for continuous beam operation, like for instance the radio-frequency (rf) quadrupole. Ion beam deposition thus inherits the advantage of chemical selectivity from MS and is therefore called preparative mass spectrometry.

Surface modification by pMS is usually approached in combination with integral surface characterization methods, like optical spectroscopy or again mass spectrometry, both in- and ex-situ.[28-32] pMS can be used for intact landing of polyatomic ions on surfaces (soft landing), inducing ion-surface reactions (reactive landing) and demonstrating effects like elastic scattering, chemical scattering, or surface induced dissociation.

Further, the capacity for surface functionalization, for instance dye attachment, catalytic activity, or enzyme immobilization, was developed.

These achievements show the great potential of pMS as a novel synthesis and investigating method capable of using large, complex molecules. However, it also confronts us with a challenge because both, the deposition process as well as the resulting surface, are highly complex. This extends the original motivation to merge pMS with SPM because this combination provides the capabilities to inspect and understand the ion-surface interactions of complex molecules.

In the following, we discuss the potential of pMS as a means of vacuum deposition of large, nonvolatile molecules, for the high resolution characterization by SPM. Preparative mass spectrometry and scanning probe microscopy make an excellent match: combined into one in-situ UHV setup, they allow us to explore the world of large, functional molecules on surfaces with unprecedented precision. We introduce the methodology of using pMS as a tool for the fabrication of well-defined molecular adsorbates of nonvolatile molecules and show examples for the structural and electronic characterization of individual macromolecules by STM and STS.

PREPARATIVE MASS SPECTROMETRY FOR SCANNING TUNNELING MICROSCOPY

The typical electrospray ion beam deposition/scanning probe microscopy (ES-IBD/SPM) experiment (sketched in Figure 1d) combines two instruments and hence two workflows. The ion beam is prepared in the MS part (left side) of the setup, starting at ambient conditions required for ESI. A variety of ion optics guides the beam through the differentially pumped vacuum system to UHV, thereby defining and characterizing its properties. The substrate, an atomically defined crystal surface, is prepared and analyzed within a surface science experiment (right side) entirely performed in UHV. The actual deposition on the surface in UHV is the link between these two workflows.

The atomically defined (metal) surface is typically prepared by repeated cycles of sputtering (e.g. Ar^+ ions, 1 keV, 10 μA, 10 min) and annealing (approx. 2/3 of the melting temperature) of a single crystal of well-defined orientation in UHV. Each surface requires its own preparation protocol. Especially procedures for semiconductor or insulator surface preparation may differ significantly. After the successful preparation is verified by SPM, the sample is transferred in-situ into the deposition stage.

In parallel, the ion beam is generated by ESI and characterized by mass spectrometry and ion current measurements. Via these measurements control over the deposition energy, the deposited ion species (molecule/fragment and charge state), and the deposition position is obtained. The ion species for deposition is selected by a m/z-filter. The kinetic energy of the beam is determined, typically by measuring deflection voltages in a retarding field geometry, which yields values for the kinetic energy per charge E_{kin}/z. The sample is biased (U_{sample}) either accelerating or decelerating the ions, defining the deposition energy

per charge as $E_d/z = E_{kin}/z - U_{sample}$. The beam is positioned on the surface by electrostatic lenses and deflection plates. During the deposition, the ion current on the sample is measured. Its integration, performed in real time during deposition, yields the deposited charge that can be converted to a molecular coverage for a known deposition area and ion charge state. Simply by switching off the ion beam once a certain charge is reached, a desired coverage can be obtained with very high precision. After deposition, the sample is transferred in-situ back to the SPM for the microscopy measurement.

The two workflows of SPM and pMS are connected in the deposition chamber of the ES-IBD instrument. Note that an in situ UHV connection is required for contamination-free sample transfer. Therefore, vacuum suitcases have been developed as an alternative, which allow to transfer samples between spatially separated, independent SPM and ES-IBD setups, while maintaining UHV conditions during the entire transfer.[33, 34]

Generally, ES-IBD setups closely resemble ESI mass spectrometers, which can be highly complex, expensive instruments, containing ion optics like lenses, ion guides, mass-filters and mass analyzers within a sophisticated, differentially pumped vacuum system.[35-37] Despite all similarities, the decisive difference of ES-IBD and ES-MS lies in the beam intensity that is required for a successful deposition or for a mass spectrum, respectively. Due to the high sensitivity and very low background in a mass spectrometer, already a few hundred ions at the detector can make for a clear peak in the spectrum, whereas 100 molecules on a macroscopic sample surface area are almost impossible to find in STM or to make an impact with respect to surface modification. For example, on a typical crystal surface area of 10 mm^2 the number of 10^9 molecules has to be deposited to find one molecule per STM scan frame of, for e.g. instance, 100 × 100 nm^2. A monolayer of a large molecule occupying 1 nm^2 surface area (e.g. C_{60}, m = 720 u) on the same surface area requires a total of $1 × 10^{13}$ molecules, which corresponds to a deposited charge of 444 pAh or 1.6 μC for singly charged ions.

Intense ion currents in the nanoampere range are thus the key requirement to achieve charges of this magnitude within a reasonable time in the order of one hour. Nowadays, ion optics like lenses, ion guides, and mass filters used in-vacuo, are performing very well optimized with respect to transmission. In particular the introduction of the rf-ion funnel[38], which effectively collimates ions entering the vacuum through the atmospheric interface into a useable ion beam, reduced the ion losses in vacuum to an extent that they are minor compared to the losses in the atmospheric interface.[39-40]

To improve the absolute ion current, pMS setups often use larger diameter inlet capillaries and compensate the increased gas load by higher pumping speed.[39-41] Leading experiments have demonstrated mass-filtered currents of up to 10 nA in high vacuum[40] or 1.5 nA in UHV (with 6 nA in HV)[39]. Recently, a hydrodynamic optimization of an nano ESI source in our lab by a funnel-shaped capillary inlet has been shown to transmit currents up to 80 nA at unity transmission to the first pumping stage of the MS vacuum system, while the same interface with a conventionally designed inlet operated at only 10% transmission.[39]

STRUCTURAL CHARACTERIZATION OF COMPLEX BIOLOGICAL MOLECULES

The three-dimensional structure of biological molecules, specifically proteins, is directly connected to their function. The precise structural characterization therefore is of utmost importance. ES-IBD as sample preparation method yields well-defined surfaces that allow for imaging by UHV-STM, which in principle offers spatial resolution at the atomic level. Applying this approach to biological molecules confronts us with the following questions: (1) Which spatial resolution can be achieved? (2) Is the primary, secondary, or ternary structure of biological molecules being influenced by the landing process? (3) What information about biological- or synthetic macromolecules can be extracted from an SPM image?

One of the first ion beam deposition experiments using gentle electrospray ionization demonstrated the intact soft-landing deposition of protein ions of low kinetic energy via the detection of the molecules in the washing solution.[42] The same experiment hinted on the retention of the native conformation when enzymatic activity was found on the prepared protein micro arrays. Similarly, the retention of helical conformations of peptides was detected after soft landing by infrared spectroscopy.[43] These successful depositions indicate the feasibility of imaging the 3d conformation of immobilized proteins or peptides prepared by pMS. Other early experiments showed that soft[36, 44, 45] or even liquid surfaces[46] are advantageous for soft landing and retention of 3d structure.

Controlling Protein Conformation on the Surface

In contrast to vapor deposition, pMS inherits the precise control of the molecular beam with respect to content, charge state, and kinetic energy from mass spectrometry. Ion mobility/mass spectrometry measurements of various proteins demonstrated that this also implies control over the conformational state in the gas phase.[23, 47-50]

To demonstrate the applicability of this control scheme, atomically flat metal surfaces were covered with protein ion beams, systematically varying the deposition parameters, and afterwards imaged by STM.[51, 52] Many deposition parameters directly influencing the adsorption conformation of the proteins on the surface were identified.

First, a native or an unfolded conformation of the protein can be selected by electrospray and solution conditions.[47, 51] Solutions of neutral pH without organic solvent contain native proteins and yield ion beams of low charge states, while unfolded proteins from acidic solutions with organic solvent will yield high charge states. This conformation selection by solvent is further supported by m/z-selection of high or low charge states. The difference between folded and unfolded proteins is directly visible in the STM micrographs. Folded proteins appear as globular features of several nm height and diameter, while unfolded proteins are imaged as extended strands (Fig. 2), sometimes backfolded in two dimensions. Due to the strong molecule-surface interaction on metal surfaces, the deposition of unfolded proteins always leads to two-dimensional (2d) structures. Thus any three-dimensional structure can only stem from the, at least partial, retention of the native 3d protein conformation after deposition.

The 2d adsorbed, unfolded strands show submolecular details whereas the 3d proteins are only imaged as one large protrusion. The resolution of SPM imaging critically depends on the shape and stability of the tip. For high aspect ratio structures like a globular protein a similarly large, high aspect ratio tip has to be well-defined and stable to yield good quality imaging, which is rather unlikely. Molecular functionalized STM or AFM tips[53-55] may further improve the resolution. In addition, methods that provide true 3d imaging, like electron holography[56] or free electron laser x-ray scattering[57] might soon reach similar resolution as STM. Also for them, a combination with pMS might be of great advantage. In all cases, the interpretation of the acquired images crucially depends on well-defined deposition of a well-know folded species.

Three experimental parameters of ES-IBD can be used independently to define the 2d conformations of unfolded proteins: surface mobility, ion charge state, and deposition energy. On strongly interacting surfaces like Cu(100), the thermal diffusion of the unfolded proteins is inhibited. When the protein is fully immobilized at room temperature, extended, random 2d conformations are observed. On less strongly interacting surfaces like Au(111) the proteins are mobile and their conformations change due to diffusion, which leads to self-interaction. Therefore at low temperatures (e.g. 40 K) the protein eventually finds a stable, local energy minimum. Observed conformations are compact, yet no uniform shape is recognizable, suggesting a randomly folded conformation.

The gas-phase charge state defines the mechanical stiffness of the polypeptide and is related to an either compact or extended gas phase conformation for high or low charge states respectively. On a surface at inhibited diffusion, e.g. Cu(100), the effect of the stiffness and gas-phase conformation on the deposition can be directly observed by STM. Upon impact the kinetic energy acts towards compacting the polymer, which is resisting by its stiffness. Stiff, high charge state proteins will be deformed less, which results in extended conformations, while soft, low charge states lead to compact, 2d-folded conformations (Fig. 2).

When the deposition energy is varied, it becomes evident that truely the interplay of stiffness and gas-phase conformation defines the adsorption conformation. The persistence length, i.e. the length on which the polymer is approximately straight, depends on the deposition energy. With higher deposition energy, the adsorption conformation of stiff, high charge state proteins becomes more compact, whereas the soft, low charge state proteins have a compact adsorption conformation already at low deposition energy and thus their persistence length does not further decrease.[52]

For the short time span of the collision event, from initial touch until the kinetic energy has dissipated, parts of the polypeptide chain are mobile even without thermal diffusion. Compact 2d conformations could also be attained by this transient mobility,
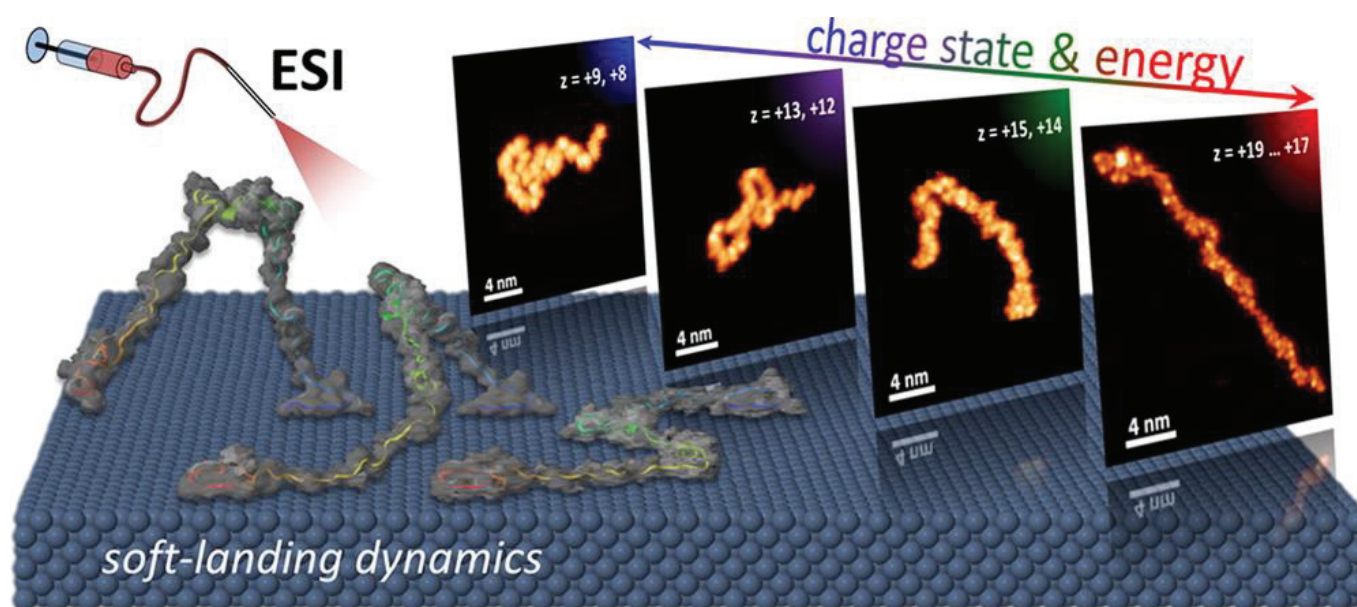
Fig. 2: Controlling the protein conformation of unfolded cytochrome c by ES-IBD. The charge state of protein ions determines the soft landing behavior. Highly charged, stiff proteins generate extended conformations. Low charge state, soft protein ions create compact structures.

which would result in compact 2d-patches similar to the structures formed by thermal diffusion.

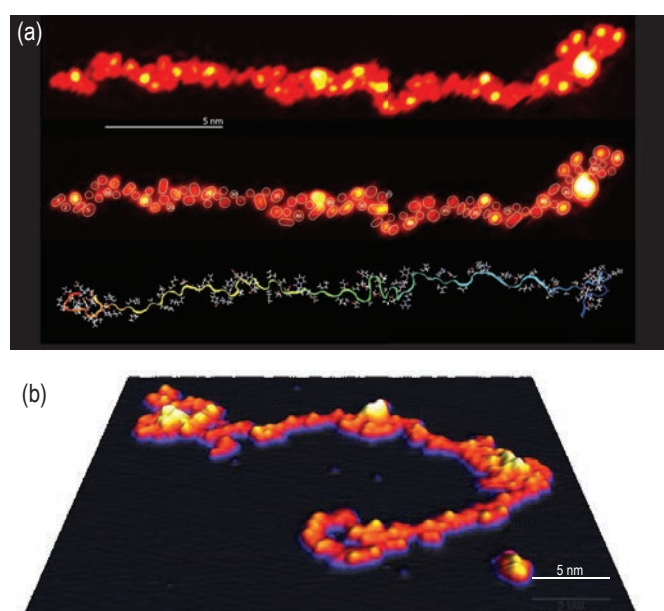## High Resolution Imaging of Proteins

Understanding the structure-function relationship and self-assembly of large molecules critically depends on the precise knowledge of their atomic structure, be it in solution or in vacuum at a surface. The capability of STM to image large molecular objects with high resolution and identify their building blocks has been demonstrated for instance for single strand DNA (ssDNA)[58] or large porphyrin nanorings[59]. In both cases the molecules were non-volatile and had to be brought onto the surface with a method alternative to evaporation. For the ssDNA a pulsed liquid inlet was used, while the porphyrine nanorings were deposited by ESD[59].

Comparing these results to the imaging of large unfolded proteins deposited by ES-IBD (Figure 3) we find that in all three cases the molecules are imaged at similar submolecular/subnanometer resolution. Their structural elements, which are the individual porphyrin units, the nuclein bases, or the amino acids, respectively, are mapped as distinguishable features. Number and symmetry of the features of the nano-ring clearly relates them to the porphyrin subunits. The DNA strand shows distinctly bright features. In an experiment with a known reference sequence, those have been related to the guanine residues of the DNA.[58]

The unfolded protein strands, of proteins of several hundred AAs, show individual protrusions of a size that fits with a single amino acid residue. Hence the vast majority of the sequence is resolved.[51] However, a complete characterization of the protein, which ultimately includes the chemical identification of the residues, is not directly possible from the STM imaging data. In contrast to the porphyrin rings, proteins do not have a high symmetry that allows for an unambiguous identification

of the features. Also unambiguously distinguishable features like the ones presented by the ss-DNA have not been found. This is not just coincidence: DNA is designed by nature to store information redundantly and make it accessible.

Proteins in contrast are chemically much more diverse than DNA. Their sequences, combined out of 20 AAs, connected via a very compact, flexible polypeptide backbone made for folding and mutual interaction – not for information storage and transfer. It is thus clear that additional symmetry or chemical information, which could support the identification of the protein residues in the STM images is not available. Even though it is possible to prepare an unfolded protein on the surface in a fully

Fig. 3: High-resolution STM imaging of proteins. Unfolded Cytochrome-c (a) and partially unfolded BSA (b) strand on Cu(100) showing features with single amino acid resolution.

extended conformation by selecting high charge states for deposition, it is likely that the same amino acids along the chain find themselves in different environments due to the self-interaction with neighboring residues and different distance and orientation towards the substrate. This results in different adsorption conformations and hence different contrast either due to different LDOS or height. Tunneling spectroscopy or imaging with modified AFM-tips[54, 60, 61] could add additional information to the image, enabling the extraction of chemical information, as outlined in the next section. For this, however, again the reduction of complexity, i.e. the investigation of short polypeptides of well defined sequence, will be the better starting point.

Folding and Sequence Controlled Self-Assembly of Peptides

For a protein like cytochrome c, which is folded in solution, a single recurring folded structure in vacuum on a metal surface can certainly not be expected. However, polypeptide chains rationally folding on surfaces might exist, but certainly have their own unique sequences that are different from proteins which fold in solution. These sequences cannot be predicted yet, but clearly the deposition of biological or other sequence controlled polymers[62] could be a promising approach for the fabrication of complex, surface based, molecular nano-structures via self-assembly. Such

approach would inherit the successful mechanisms of biological molecules, for instance sequence encoded structures[63] from folding, or functionality by molecular recognition[64] by induced fits. A reduction of complexity, i.e. the study of small polypeptides will be a promising starting point, for this goal as well.

Indeed, very recently, the formation of stable molecular nanostructures via two-dimensional folding of the nine AA peptide bradykinin (BK)[65] and sequence controlled self-assembly of angiotensin peptides (angiotensin-I and -II, At-I, At-II)[66] has been investigated by STM supported by computer simulations.

The peptides At-II deposited on the gold surface did not yield highly ordered structures. Only short, periodic arrangements of three to five dimers or small patches or molecules stacked in row were found. Elucidation of their structure with the help of molecular dynamics simulations showed that a bend at the C-terminal inhibited efficient binding in the dimer and further masked the attachment of a neighboring structure. The removal of two amino acids at the C-terminal changed the behavior thus completely. Now, large, highly ordered domains of a chiral hexagon structure are found. The walls of the network are peptides arranged in dimers, three of which are connected in vortices to form the characteristic honeycomb-like shape. Clearly, small changes in the AA-sequence command the assembly of the molecule.
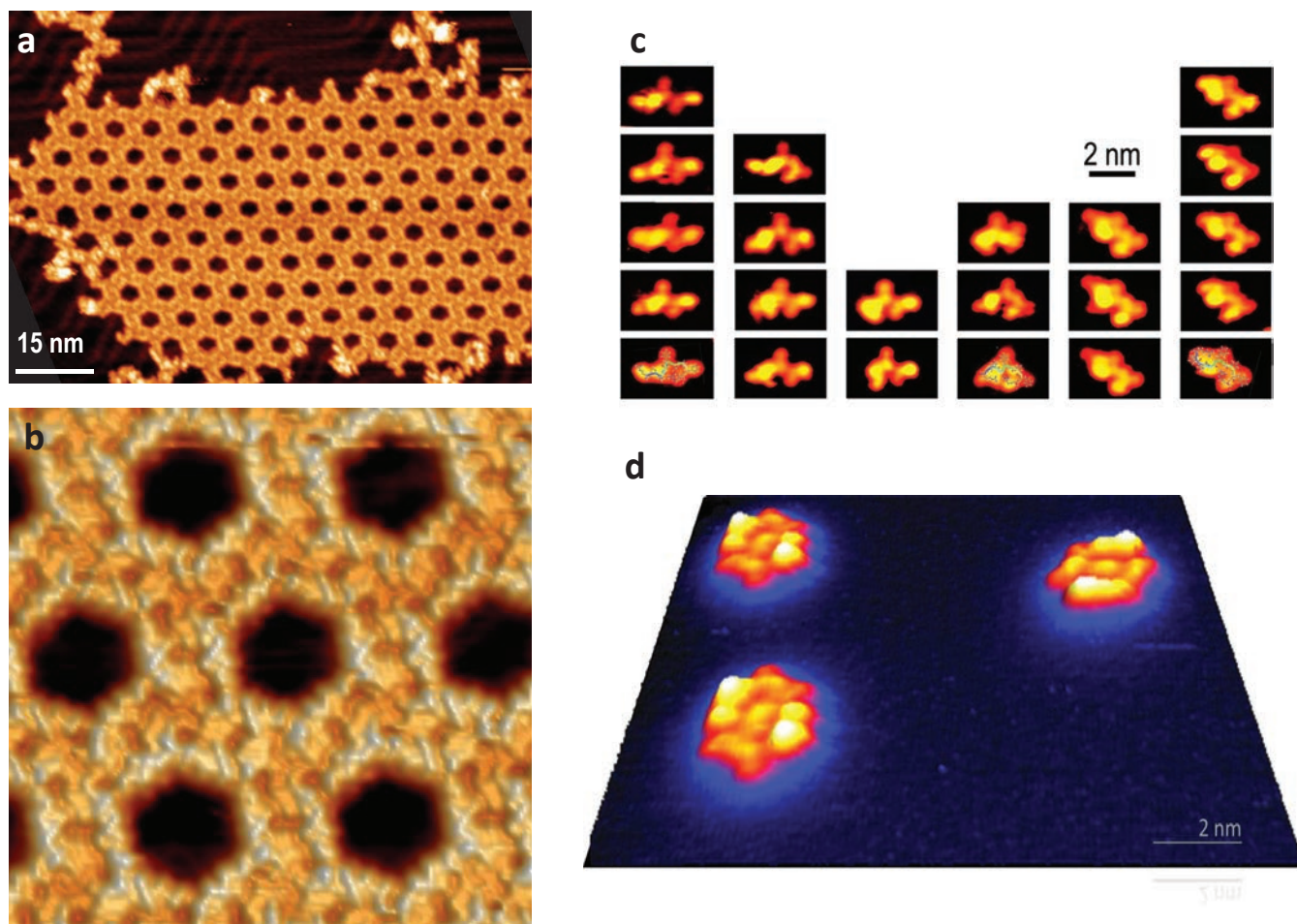
Fig. 4: Nanostructures of peptides imaged by STM. (a) Survey image of the highly ordered, chiral, molecular network of angiotensin-II on Au(111). (b) Magnified view of the At-II network. (c) Conformational variability of the peptide bradykinin observed on a Cu(110) surface where it is fully immobilized at room temperature. (d) Surface mobility allows for the formation of one well-defined dimer nanostructure of BK on Cu(100) at RT.

Besides sequence control, folding is the other major property of biological polypeptides, as it allows for the fabrication of functional nanostructures from a universal synthesis which follows a plan encoded in the DNA. The code thus not only contains the structure and conformation of the functional molecules, but also the pathway to reach it. Choosing tht flexible peptide, bradykinin (BK) we were able to demonstrate the conformational flexibility when we deposit it to a very sticky surface (Cu(110)). Completely immobilized upon deposition, many different structures are observed, indicative of a variety of conformations, which can be grouped in conformation classes. (see Fig. 4c). If the molecule is given the freedom to diffuse and rearrange, suddenly only one molecular nanostructure is found: a dimer of two BK molecules. The analysis of the conformation of this dimer shows that in it BK takes a very compact conformation to accommodate two specific bonds sites to the partner molecule. These specific bonds in turn stabilize the binding, a principle which in biology is called induced fit binding. Further, hydrophobic and hydrophilic groups in the molecule segregate. Also this is typical for biological molecules, however in vacuum the segregation occurs inverted with polar molecules at the inside and nonpolar molecules at the outside, an effect which we observed several times in our experiments.[66, 67] The consequence however is similar. Presenting the non-interacting unpolar groups at the rim passivates the dimers and hinders unspecific interaction, which would destabilize the structure.

With the observations of sequence control and inverted, two-dimensional folding of polypeptides on surfaces a new way of generating functional nanostructures presents itself. Being compatible with vacuum technology, it inherits the advantages from biology, which are the tunability of the structure through the sequence and an universal synthesis of the molecule, independent from the final function. The grand challenge that remains is finding useful codes in the endless space of amino acid sequences, for which we cannot rely on biological evolution, but have to understand the structure formation on the atomic level, for which STM is the best tool available.

SPECTROSCOPIC INVESTIGATIONS OF FUNCTIONAL MOLECULES

One of the most fascinating strengths of SPM is its capability to detect physical and chemical properties with resolution down to the submolecular level by performing spectroscopic measurements. In this context, bias spectroscopy in an STM is the most commonly used spectroscopic mode, in which the differential junction conductance dI/dV versus the applied bias voltage V is recorded, while the probing tip rests statically at the point of interest. The differential conductance directly measures the tunneling probability at the applied bias and is proportional to the convolution of the local density of states (LDOS) in tip and sample[68, 69]. By characterizing the tip's LDOS, this method enables the direct access to such fundamental properties as the energy of molecular orbitals and their interaction with the substrate electrons.

Additionally, tunneling electrons with sufficient energy can locally probe vibronic or magnetic excitations on the surface or in

adsorbate atoms and molecules. The increased tunneling probability when inelastic channels open at the bias voltage corresponding to the energy of the excitation leaves characteristic, usually bias symmetric, leads to steps in the dI/dV or equivalent peak-dip structures in the second derivative of the current (dI^2/d^2V).[11, 70] At low temperatures the energy resolution is sufficient to distinguish between different isotopes in molecules due to the shift in bond vibration with atomic mass.[11, 71, 72]

Since the advent of SPM, many other spectroscopy modes have been employed to locally resolve for example the apparent barrier height by measuring the current decay vs. tip-sample separation[73] or to determine lifetimes of excitations by
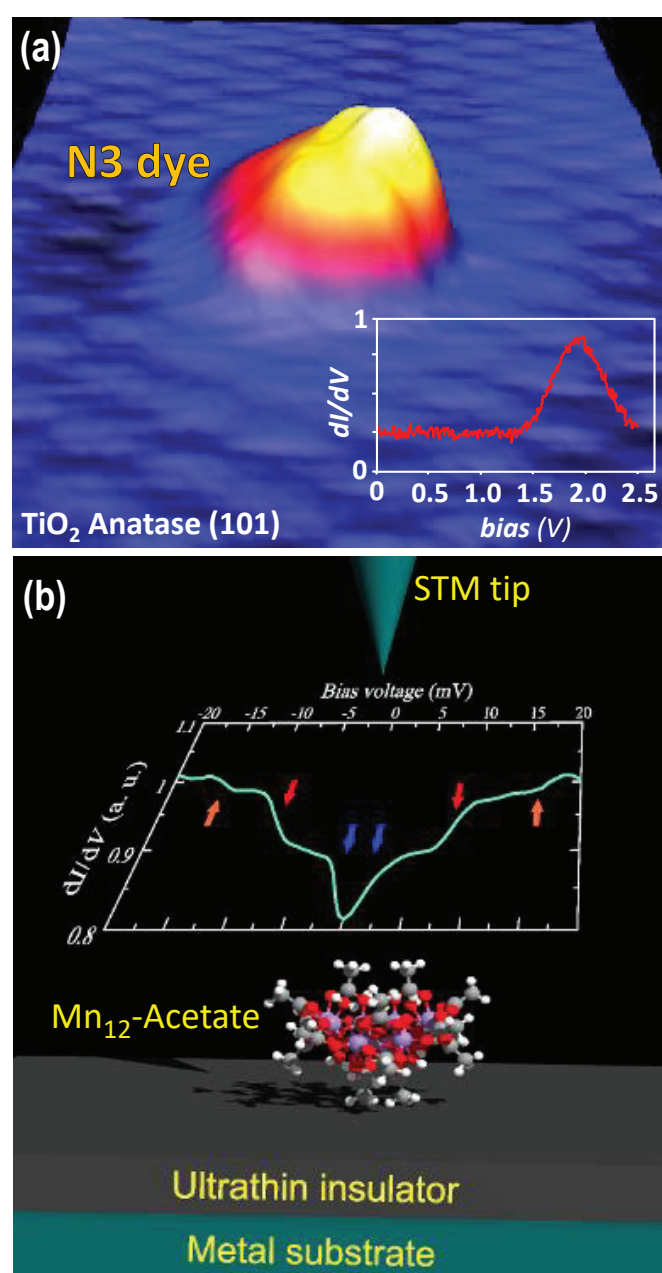
Fig. 5: Examples of scanning tunneling spectroscopy (STS) measurements on ES-IBD grafted molecules on surfaces.[34] (a) Topographic image of Ru based N3 dye molecule on TiO₂ anatase with characteristic tunneling spectrum. (b) Tunneling spectrum of individual Manganese-12-Acetate-16 molecules adsorbed on the monoatomic h-BN/Rh(111) surface showing magnetic excitations.[33]

pump-probe methods[74-76]. Here, the non-contact AFM with its access to the forces acting between tip and sample allows to extend the spectroscopic possibilities dramatically: by integrating force-distance curves the atomic scale interaction potentials are measured directly[5, 77], by minimizing the interacting forces with an applied bias, local Kelvin probe spectroscopy is performed, or surface charges are directly mapped.[61]

The capabilities of ES-IBD allow to use local spectroscopy now on individual, large, nonvolatile molecules. Figure 5a shows a high resolution STM image of the ruthenium based N3 dye molecule (cis-di(thiocyanato)-bis(2,2′-bipyridyl-4,4′-dicarboxylate) ruthenium(II)) on the TiO$_2$-anatase surface after ES-IBD preparation.[34] These molecules are widely used in dye sensitized solar cells, however, within a solar cell, the access to the electronic properties of the individual dye molecules is impossible. On the anatase surface multiconformational binding is detected in STM, seen by the different appearance of each molecule. These different adsorption geometries influence the position of the lowest unoccupied molecular orbital LUMO strongly as seen directly in the wide spread of the band's onset in STS.

Figure 5b shows Manganese-12-Acetate-16 molecules, an archetypical single molecular magnet with high intrinsic spin and long spin relaxation time[78]. In our experiments they were adsorbed on Au(111) and h-BN:Rh(111). Observing the characteristic shape of the molecule by STM reveals the capacity of ES-IBD, which permits the preparation of this infamously fragile molecule.[79] However, in the STM topography the molecule appears on both substrates intact, while only STS reveals that the molecule loses its magnetic properties on the Au surface due to the coupling of the molecular states with the states of the metal.[80] Contrary, on the ultra-thin decoupling layer h-BN:Rh(111) low energy excitations are observed (Fig. 5b). Calculating the spin-flip transition probabilities[81] of this complex coupled system with a ground state total spin of S = 10 allows to identify the observed transitions as an energetically low lying excitation which changes only the magnetic quantum number and two excitations at higher energy which additionally changes the total spin from S = 10 to S = 9, clearly demonstrating an intact magnetic core.[33]

Note, this experiment is only possible in a low temperature (1K) STM using ES-IBD for preparation and a vacuum suitcase for linking the two instruments. This was the first time a molecular magnet was accessed as an individual molecule on the surface, which perfectly underlines the relevance of the ES-IBD/SPM combination. Extrapolating the developments in synthetic chemistry and molecular nanoscience leads to even larger, multifunctional molecules or biomimetic systems like sequence controlled polymers. In these systems locally addressing functions and relating them to structure, while maintaining chemical control over the environment will be extremely important, for which local probe spectroscopy may be a crucial tool.

CONCLUSION AND OUTLOOK

The preparation of ultrapure, atomically defined surfaces is a new application of preparative mass spectrometry with great prospects. In principle, the well-defined preparation of a sample is useful for any (surface science) characterization method. It is thus not very surprising that pMS was used successfully in combination with many other surface analysis methods such a secondary ionization mass spectrometry[82, 83], infrared spectroscopy,[43] Raman spectroscopy[84, 85], or electrochemistry[86].

Nevertheless, we think that single molecule methods have a special role as only they can fully exploit the high degree of control and purity that ES-IBD offers. The chemical selectivity from mass spectrometry combined with the high spatial resolution of a single particle allows for accessing its complexity without losing spatial precision, opening the road to investigations of individual, functional, and macromolecules.

The perspective for ES-IBD/SPM is highly interesting for fundamental research, especially for biological model systems, be it proteins, peptides, glycans, or molecules of synthetic origin. Certainly the interactions on a surface in vacuum will be different from those in aqueous environment, which is particularly relevant for biology. Nevertheless, the complexity of the interactions prevails and fundamental aspects like folding or sequence controlled assembly seem feasible as well in vacuum. In fact, surface based studies in vacuum do not exclude the possibility to investigate the role of solvents at the molecular scale.[87] Furthermore, the chemistry of ions at the surface, especially in collisions at hyperthermal energy, holds prospects
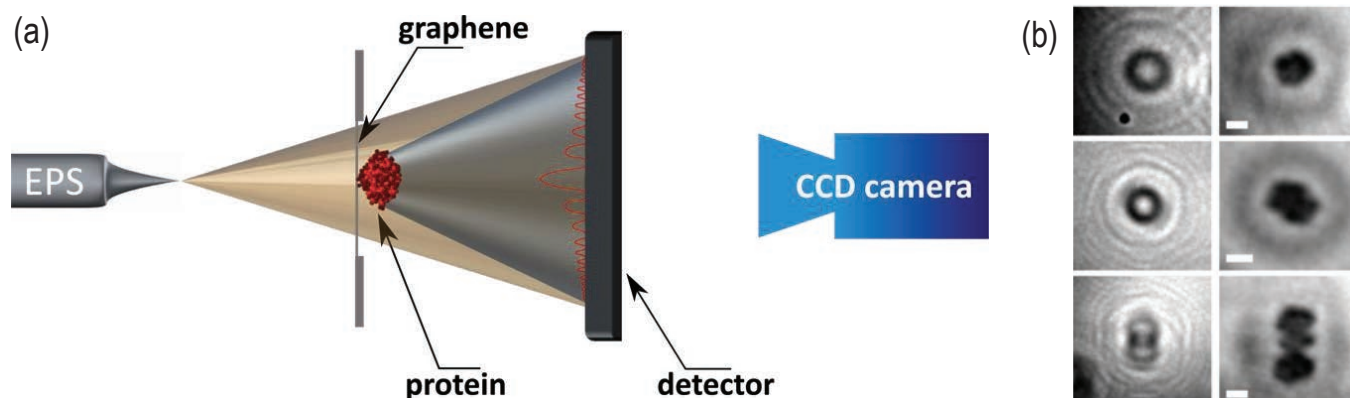
Fig. 6: Low energy electron holography. (a) Scheme of the low energy electron holography experiment. (b) Hologram and reconstruction of an individual cytochrome c protein as well as a dimer and trimer, deposited on a freestanding monolayer graphene membrane as folded protein ion by soft-landing electrospray ion beam deposition.[94]
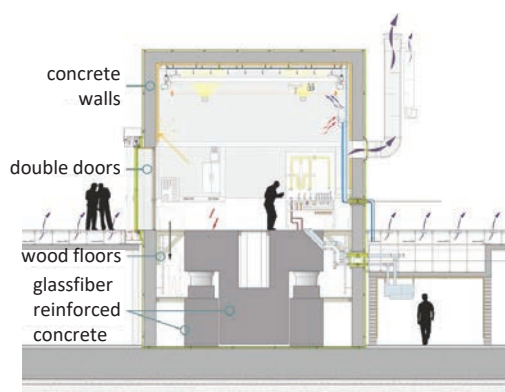
worthwhile being investigated, both from chemical and morphological point of view.[35, 85, 88, 89]

A very interesting perspective is opened by applying transparent substrates which become available by the advent of two-dimensional materials.[90] In a collaborative effort with J.N. Longchamp and H.W. Fink of the University of Zurich we were able to deposit native proteins on ultraclean freestanding graphene[91] and use our UHV-suitcase technology to transport them to a novel low-energy, electron holography microscope,[56, 92] realizing Denis Gabors idea for electron holography.[93] The samples to be studied are presented to a highly coherent beam of low-energy electrons generated by an atomically sharp field emitter tip placed as close as 100 nm in front of the sample. The interference pattern formed by the scattered and unscattered electron waves, the so-called hologram, is recorded by a multi channel plate electron detector at several centimeters distance. Subsequent numerical hologram reconstruction involving back propagation of the wave

front from the hologram to the sample plane reveals the structure of the object under study. Operating at electron energies at 50-150 eV this instrument avoids radiation damage and already at the present resolution of 7 Å the shape of a single protein can be imaged (Fig. 6).[94] The performance of the method is currently only limited by mechanical vibrations, and hence it could become an important tool for structural biology, in particular since analytical mass spectrometry recently unlocked the realm of native gas phase proteins by reliably ionizing intact folded soluble protein, membrane proteins and protein complexes.[95, 96] In contrast to the current state-of-the-art in structural biology, we do not need averaging over many molecules. This achievement constitutes a major step towards structural biology at a truly single molecule level; a vision that has often been subject of discussions and speculations and a long-standing dream.

There is no fundamental limit in reaching true atomic resolution. The limiting factor is essentially the susceptibility of high-


concrete walls

double doors

wood floors

glassfiber reinforced concrete

vibrational level: < 10 nm/s

acoustic shielding: 60 dB

electromagnetic shielding: 100 dB

Fig. 7: Precision Laboratory (PL) at the MPI for Solid State Research in Stuttgart. The PL is a large isolated experiment hall partially enclosed by an office/service lab wing. The hall comprises eleven individually decoupled experiments. Each experiment is seismically, acoustically, and electromagnetically shielded from the environment. In order to technically realize these experimental environments, the challenges in the construction of the new laboratory pushed the technical limits and set new standards. A concrete box with a 60 dB attenuation encapsulates each experiment to acoustically isolate it from the immediate laboratory environment. External vibrations are dampened by a massive concrete block inside the acoustic box weighing between 100 t and 190 t. Set on air springs, vibrations are reduced to a level of <10 nm/s, several orders of magnitude smaller than the best industry standard today. For experiments operating at temperatures below 100 mK, the acoustic boxes are electromagnetically shielded by a closed metal shell yielding 100 dB attenuation. Further, the building has been constructed such that the general noise sources have been reduced as well. This includes, but is not limited to separate acoustic boxes at each experiment for noisy equipment, such as roughing pumps, shielded power lines, all optical data network and correspondingly all optical voice-over-IP telecommunication.

order interference fringes to mechanical vibrations. The Precision Laboratory at the Max-Planck Institute in Stuttgart offers the unique environment needed to beat the odds and reach the goal of atomic resolution (Fig. 7). The Laboratory was built on the initiative of one of the authors (KK) between 2008 and 2012 and has set new standards for noise-free environments, and the low-energy electron projection holography does profit enormously from these exceptional conditions. We are currently developing jointly a cryogenic low-energy electron based holography microscope which should be able to "image" individual molecules and nanostructures with atomic resolution.

Taking full advantage of the Stuttgart Precision Laboratory we have created cutting edge experimental set-ups with a focus on lowest energy phenomena at the atomic scale encompassing highest energy resolution and the introduction of pump-probe schemes to access ultra-fast dynamics. With a spectroscopic resolution of 11 µeV our Millikelvin-STM currently holds the world record. [97] An important breakthrough was the study of the Josephson effect with this unique instrument. At these extremely low temperatures, the electrons reveal their full quantum nature. The electric current is therefore a granular medium, consisting of individual particles. The electrons trickle through a conductor like grains of sand in an hourglass, a phenomenon that can be explained with the aid of quantum electrodynamics.[98] These developments open up new avenues to explore light matter interaction on the atomic scale (Fig. 8a), e.g. the possibility to use nanoscale Josephson junctions as a source and detector of radiation in the upper Gigahertz regime directly built into the tunneling junction.[99]

Converting photon energy into electrical energy and vice-versa is a key process in energy and information technology. We are exploring novel approaches to control energy conversion and transduction at surfaces on the single molecule level. Charge injection processes were directly addressed by STM-controlled electroluminescence at selected structural defects on thin fullerene films. In this configuration we realized an anti-correlated single photon source for the first time within the STM tunnel junction and were thus able to locally measure and manipulate picosecond exciton life times.[100] Using the fullerene film as a decoupling layer for isolated organic admolecules we demonstrated the function of a prototypical plasmon and light-emitting transistor (Fig. 8b). The electrostatic potential of a decoupled single fac-tris(2-phenylpyridine)iridium(III) molecule was controlled with millivolt precision which allows tuning the local tunnel current and the light emission intensity over sev-
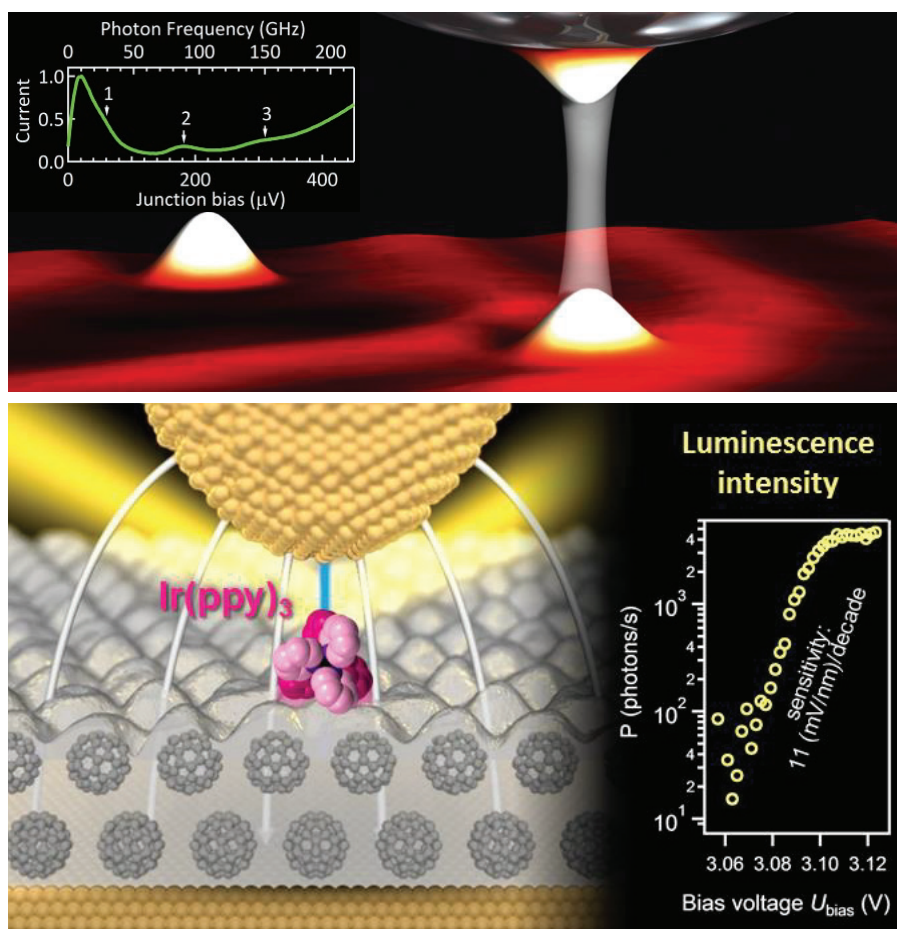
Fig. 8: Advanced Scanning Probe Microscopy and Spectroscopy. (a) With the record resolution of our Millikelvin-STM we have been able to lay the foundations for the successful exploration of Josephson Scanning Tunneling Microscopy. (b) The Single Molecule Plasmon Emitting Field-Effect Transistor using a single fac-tris(2-phenylpyridine)iridium(III) molecule is the smallest device controlling light emission and electrical current simultaneously with GHz switching rates.

eral orders of magnitude. Transition times between the transistor's on- and off-state were faster than one nanosecond. [101] The key experimental development that provided access to charge excitation dynamics on the atomic scale with picosecond resolution is time-resolved scanning tunneling fluorescence. To this end we employed the light emission from the STM to determine the precise shape of STM voltage pulses with picosecond resolution and millivolt precision inside the tunnel junction. The well-characterized short voltage pulses thus obtained were then employed to explore the charge transfer dynamics of single molecules with unprecedented spatio-temporal resolution.

Future scientific projects will combine the capabilities of ES-IBD with the high performance scanning probe techniques operated in the PL. Particular fascinating is the possibility to create complex molecular nanostructures at surfaces with properties determined by quantum behavior on one hand and approaching functionalities of living matter on the other hand.

This article is in part based on the extended review article "Mass Spectrometry as a Preparative Tool for the Surface Science of Large Molecules" in Annual Reviews of Analytical Chemistry 2016.[27]

REFERENCES

[1] J. V. Barth, G. Costantini, and K. Kern, *Nature* **437**, 671 (2005).

[2] G. Binnig, C. F. Quate, and C. Gerber, *Phys. Rev. Lett.* **56**, 930 (1986).

[3] G. Binnig and H. Rohrer, *Rev. Mod. Phys.* **59**, 615 (1987).

[4] J. A. Stroscio and D. M. Eigler, *Science* **254**, 1319 (1991).

[5] M. Ternes, C. P. Lutz, C. F. Hirjibehedin, F. J. Giessibl, and A. J. Heinrich, *Science* **319**, 1066 (2008).

[6] G. Binnig, H. Rohrer, C. Gerber, and E. Weibel, *Phys. Rev. Lett.* **50**, 120 (1983).

[7] F. J. Giessibl, *Science* **267**, 68 (1995).

[8] J. Tersoff and D. Hamann, *Phys. Rev. Lett.* **50**, 1998 (1983).

[9] F. J. Giessibl, *Rev. Mod. Phys.* **75**, 949 (2003).

[10] H. J. Zandvliet and A. van Houselt, *Annual Review of Analytical Chemistry* **2**, 37 (2009).

[11] B. C. Stipe, M. A. Rezaei, and W. Ho, *Science* **280**, 1732 (1998).

[12] C. F. Hirjibehedin, C. P. Lutz, and A. J. Heinrich, *Science* **312**, 1021 (2006).

[13] C. F. Hirjibehedin, C.-Y. Lin, A. F. Otte, M. Ternes, C. P. Lutz, B. A. Jones, and A. J. Heinrich, *Science* **317**, 1199 (2007).

[14] L. Vitali, G. Levita, R. Ohmann, A. Comisso, A. De Vita, and K. Kern, *Nat. Mater.* **9**, 320 (2010).

[15] A. Della Pia, M. Riello, A. Floris, D. Stassen, T. S. Jones, D. Bonifazi, A. De Vita, and G. Costantini, *ACS Nano* **8**, 12356 (2014).

[16] F. Mohn, L. Gross, N. Moll, and G. Meyer, *Nat. Nanotechnol.* **7**, 227 (2012).

[17] L. Gross, N. Moll, F. Mohn, A. Curioni, G. Meyer, F. Hanke, and M. Persson, *Phys. Rev. Lett.* **107**, 086101 (2011).

[18] M. Dole, L. L. Mack, R. L. Hines, R. C. Mobley, L. D. Ferguson, and M. B. Alice, *J. Chem. Phys.* **49**, 2240 (1968).

[19] M. Karas, D. Bachmann, and F. Hillenkamp, *Analytical Chemistry* **57**, 2935 (1985), http://pubs.acs.org/doi/pdf/10.1021/ac00291a042.

[20] J. B. Fenn, M. Mann, C. K. Meng, S. F. Wong, and C. M. Whitehouse, *Science* **246**, 64 (1989).

[21] A. Dongre, A. Somogyi, and V. Wysocki, *J. Mass Spectrom.* **31**, 339 (1996), ISSN 1076-5174.

[22] S. W. Englander, *J. Am. Soc. Mass Spectrom.* **17**, 1481 (2006).

[23] B. C. Bohrer, S. I. Merenbloom, S. L. Koeniger, A. E. Hilderbrand, and D. E. Clemmer, *Annu Rev of Anal Chem* **1**, 293 (2008).

[24] E. V. Petrotchenko and C. H. Borchers, *Mass Spectrom. Rev.* **29**, 862 (2010).

[25] N. A. Pierson, L. Chen, S. J. Valentine, D. H. Russell, and D. E. Clemmer, *J. Am. Chem. Soc.* **133**, 13810 (2011), ISSN 0002-7863.

[26] F. Herzog, A. Kahraman, D. Boehringer, R. Mak, A. Bracher, T. Walzthoeni, A. Leitner, M. Beck, F.-U. Hartl, N. Ban, et al., *Science* **337**, 1348 (2012).

[27] S. Rauschenbach, M. Ternes, L. Harnau, and K. Kern, *Annu. Rev. Anal. Chem.* **9**, 16.1 - 16.26 (2016).

[28] R. G. Cooks, S. C. Jo, and J. Green, *Appl. Surf. Sci.* **231-2**, 13 (2004).

[29] G. E. Johnson, Q. Hu, and J. Laskin, *Annu. Rev. Anal. Chem.* **4**, 83 (2011).

[30] J. Cyriac, T. Pradeep, H. Kang, R. Souda, and R. G. Cooks, *Chem. Rev.* **112**, 5356 (2012), ISSN 0009-2665.

[31] G. Verbeck, W. Hoffmann, and B. Walton, *Analyst* **137**, 4393 (2012).

[32] G. E. Johnson, D. Gunaratne, and J. Laskin, *Mass Spectrom. Rev. 00*, **1** (2015).

[33] S. Kahle, Z. Deng, N. Malinowski, C. Tonnoir, A. Forment-Aliaga, N. Thontasen, G. Rinke, D. Le, V. Turkowski, T. S. Rahman, et al., *Nano Lett.* **12**, 518 (2012).

[34] C. S. Kley, C. Dette, G. Rinke, C. E. Patrick, J. Cechal, S. J. Jung, M. Baur, M. Dürr, S. Rauschenbach, F. Giustino, et al., *Nano Lett.* **14**, 563 (2014).

[35] V. Grill, J. Shen, C. Evans, and R. G. Cooks, *Rev. Sci. Instrum.* **72**, 3149 (2001).

[36] J. Alvarez, R. G. Cooks, S. E. Barlow, D. J. Gaspar, J. H. Futrell, and J. Laskin, *Anal. Chem.* **77**, 3452 (2005).

[37] S. Rauschenbach, F. L. Stadler, E. Lunedei, N. Malinowski, S. Koltsov, G. Costantini, and K. Kern, *Small* **2**, 540 (2006).

[38] R. T. Kelly, A. V. Tolmachev, J. S. Page, K. Tang, and R. D. Smith, *Mass Spectrometry Reviews* **29**, 294 (2010).

[39] M. Pauly, M. Sroka, J. Reiss, G. Rinke, A. Albarghash, R. Vogelgesang, H. Hahne, B. Kuster, J. Sesterhenn, K. Kern, et al., *Analyst* **139**, 1856 (2014).

[40] K. D. D. Gunaratne, V. Prabhakaran, Y. M. Ibrahim, R. V. Norheim, G. E. Johnson, and J. Laskin, *Analyst* **140**, 2957 (2015).

[41] M. Volny and F. Turecek, *J. Mass Spectrom.* **41**, 124 (2006).

[42] Z. Ouyang, Z. Takats, T. A. Blake, B. Gologan, A. J. Guymon, J. M. Wiseman, J. C. Oliver, V. J. Davisson, and R. G. Cooks, *Science* **301**, 1351 (2003).

[43] P. Wang and J. Laskin, *Angew. Chem., Int. Ed.* **47**, 6678 (2008).

[44] S. A. Miller, H. Luo, S. J. Pachuta, and R. G. Cooks, *Science* **275**, 1447 (1997).

[45] H. Luo, S. A. Miller, R. G. Cooks, and S. J. Pachuta, *International Journal of Mass Spectrometry* **174**, 193 (1998).

[46] B. Gologan, Z. Takats, J. Alvarez, J. M. Wiseman, N. Talaty, Z. Ouyang, and R. G. Cooks, *J. Am. Soc. Mass Spectrom.* **15**, 1874 (2004).

[47] D. E. Clemmer, R. R. Hudgins, and M. F. Jarrold, *J. Am. Chem. Soc.* **117**, 10141 (1995).

[48] K. B. Shelimov, D. E. Clemmer, R. R. Hudgins, , and M. F. Jarrold, *J. Am. Chem. Soc.* **119**, 2240 (1997).

[49] C. S. Hoaglund-Hyzer, A. E. Counterman, and D. E. Clemmer, *Chemical Reviews* **99**, 3037 (1999), 341.

[50] T. Wyttenbach, N. A. Pierson, D. E. Clemmer, and M. T. Bowers, *Annual review of physical chemistry* **65**, 175 (2014).

[51] Z. Deng, N. Thontasen, N. Malinowski, G. Rinke, L. Harnau, S. Rauschenbach, and K. Kern, *Nano Lett.* **12**, 2452 (2012).

[52] G. Rinke, S. Rauschenbach, L. Harnau, A. Albarghash, M. Pauly, and K. Kern, *Nano Lett.* **14**, 5609 (2014).

[53] L. Gross, F. Mohn, N. Moll, B. Schuler, A. Criado, E. Guitian, D. Pena, A. Gourdon, and G. Meyer, *Science* **337**, 1326 (2012).

[54] C. Weiss, C. Wagner, C. Kleimann, M. Rohlfing, F. S. Tautz, and R. Temirov, *Phys. Rev. Lett.* **105**, 086103 (2010).

[55] P. Hapala, R. Temirov, F. S. Tautz, and P. Jelinek, *Phys. Rev. Lett.* **113**, 226101 (2014).

[56] J.-N. Longchamp, T. Latychevskaia, C. Escher, and H.-W. Fink, *Phys. Rev. Lett.* **110**, 255501 (2013).

[57] H. N. Chapman, P. Fromme, A. Barty, T. A. White, R. A. Kirian, A. Aquila, M. S. Hunter, J. Schulz, D. P. DePonte, U. Weierstall, et al., *Nature* **470**, 73 (2011), ISSN 0028-0836.

[58] H. Tanaka and T. Kawai, *Nature Nanotechnology* **4**, 518 (2009).

[59] M. C. O'Sullivan, J. K. Sprafke, D. V. Kondratuk, C. Rinfray, T. D. W. Claridge, A. Saywell, M. O. Blunt, J. N. O'Shea, P. H. Beton, M. Malfois, et al., *Nature* **469**, 72 (2011).

[60] C. Wagner and R. Temirov, *Prog. Surf. Sci.* **90**, 194 (2015).

[61] L. Gross, F. Mohn, P. Liljeroth, J. Repp, F. J. Giessibl, and G. Meyer, *Science* **324**, 1428 (2009).

[62] J.-F. Lutz, M. Ouchi, D. R. Liu, and M. Sawamoto, *Science* **341**, 1238149 (2013).

[63] C. M. Goodman, S. Choi, S. Shandler, and W. F. DeGrado, *Nature chemical biology* **3**, 252 (2007).

[64] M. Lingenfelder, G. Tomba, G. Costantini, L. C. Ciacchi, A. De Vita, and K. Kern, *Angew. Chem., Int. Ed.* **46**, 4492 (2007).

[65] S. Rauschenbach, G. Rinke, R. Gutzler, S. Abb, A. Albargash, D. Le, T. Rahman, M. Dürr, L. Hanau, and K. Kern, *ACS Nano*, doi: 10.1021/acsnano.6b06145 (2017).

[66] S. Abb, L. Harnau, R. Gutzler, S. Rauschenbach, and K. Kern, *Nature Communications* **7**, 10335 (2016).

[67] S. Rauschenbach, G. Rinke, N. Malinowski, R. T. Weitz, R. Dinnebier, N. Thontasen, Z. Deng, T. Lutz, P. M. de Almeida Rollo, G. Costantini, et al., *Adv. Mater.* **24**, 2761 (2012).

[68] J. Tersoff and D. R. Hamann, *Phys. Rev. B* **31**, 805 (1985).

[69] N. D. Lang, *Phys. Rev. B* **34**, 5947 (1986).

[70] A. J. Heinrich, J. A. Gupta, C. P. Lutz, and D. M. Eigler, *Science* **306**, 466 (2004).

[71] A. J. Heinrich, C. P. Lutz, J. A. Gupta, and D. M. Eigler, *Science* **298**, 1381 (2002).

[72] F. D. Natterer, F. Patthey, and H. Brune, *Phys. Rev. Lett.* **111**, 175303 (2013).

[73] L. Vitali, G. Levita, R. Ohmann, A. Comisso, A. De Vita, and K. Kern, *Nature Materials* **9**, 320 (2010).

[74] S. Loth, M. Etzkorn, C. P. Lutz, D. M. Eigler, and A. J. Heinrich, *Science* **329**, 1628 (2010).

[75] C. Grosse, M. Etzkorn, K. Kuhnke, S. Loth, and K. Kern, *Appl. Phys. Lett.* **103**, 183108 (2013).

[76] S. Yan, D.-J. Choi, J. A. J. Burgess, S. Rolf-Pissarczyk, and S. Loth, *Nature Nanotechnology* **10**, 40 (2015).

[77] H. Holscher, S. M. Langkat, A. Schwarz, and R. Wiesendanger, *Appl. Phys. Lett.* **81**, 4428 (2002).

[78] R. Sessoli, D. Gatteschi, A. Caneschi, and M. A. Novak, *Nature* **365**, 141 (1993).

[79] M. Mannini, F. Pineider, P. Sainctavit, C. Cartier dit Moulin, M.-A. Arrio, A. Cornia, D. Gatteschi, and R. Sessoli, *The European Physical Journal - Special Topics* **169**, 167 (2009).

[80] M. Mannini, P. Sainctravit, R. Sessoli, C. C. dit Moulin, F. Pineider, M.-A. Arrio, A. Cornia, and D. Gatteschi, *Chem. Eur. J.* **14**, 7530 (2008).

[81] M. Ternes, *New J. Phys.* **17**, 063016 (2015).

[82] S. Rauschenbach, R. Vogelgesang, N. Malinowski, J. W. Gerlach, M. Benyoucef, G. Costantini, Z. Deng, N. Thontasen, and K. Kern, *ACS Nano* **3**, 2901 (2009).

[83] Z. Nie, G. Li, M. P. Goodwin, L. Gao, J. Cyriac, and R. G. Cooks, *J. Am. Soc. Mass Spectrom.* **20**, 949 (2009).

[84] J. Cyriac, M. Wleklinski, G. Li, L. Gao, and R. G. Cooks, *Analyst* **137**, 1363 (2012).

[85] G. Dubey, R. Urcuyo, S. Abb, G. Rinke, M. Burghard, S. Rauschenbach, and K. Kern, *J. Am. Chem. Soc.* **136**, 13482 (2014).

[86] F. Pepi, A. Tata, S. Garzoli, P. Giacomello, R. Ragno, A. Patsilinakos, M. D. Fusco, A. D'Annibale, S. Cannistraro, C. Baldacchini, et al., *The Journal of Physical Chemistry C* **115**, 4863 (2011).

[87] Y. Chen, K. Deng, X. Qiu, and C. Wang, *Scientific reports* **3** (2013).

[88] A. Li, Q. Luo, S.-J. Park, , and R. G. Cooks, *Angew. Chem* **126**, 3211 (2014).

[89] G. Rinke, S. Rauschenbach, S. Schrettl, T. N. Hoheisel, J. Blohm, R. Gutzler, F. Rosei, H. Frauenrath, and K. Kern, *Int. J. Mass. Spectrom.* **377**, 228 (2015), (100 Years of Mass Spectrometry Special Edition).

[90] A. K. Geim and K. S. Novoselov, *Nature Materials* **6**, 183 (2007).

[91] J.-N. Longchamp, C. Escher, and H.-W. Fink, *J. Vac. Sci. Technol. B* **31**, 020605 (2013).

[92] T. Latychevskaia, J.-N. Longchamp, C. Escher, and H.-W. Fink, *Ultramicroscopy* **159**, 395 (2015).

[93] D. Gabor, *Nature* **161**, 777 (1948).

[94] J.-N. Longchamp, S. Rauschenbach, S. Abb, C. Escher, T. Latychevskaia, K. Kern, and H.-W. Fink, *Proc. Natl. Acad. Sci. USA*, doi: 10.1073/pnas.1614519114 (2017).

[95] N. P. Barrera, N. Di Bartolo, P. J. Booth, and C. V. Robinson, *Science* **321**, 243 (2008).

[96] J. T. Hopper, Y. T.-C. Yu, D. Li, A. Raymond, M. Bostock, I. Liko, V. Mikhailov, A. Laganowsky, J. L. Benesch, M. Caffrey, et al., *Nature methods* **10**, 1206 (2013).

[97] M. Assig, M. Etzkorn, A. Enders, W. Stiepany, C. R. Ast, and K. Kern, Review of *Scientific Instruments* **84**, 033903 (2013).

[98] C. R. Ast, B. Jck, J. Senkpiel, M. Eltschka, M. Etzkorn, J. Ankerhold, and K. Kern, *Nature Communications* **7**, 13009 (2016).

[99] M. Eltschka, B. Jck, M. Assig, O. V. Kondrashov, M. A. Skvortsov, M. Etzkorn, C. R. Ast, and K. Kern, *Appl. Phys. Lett.* **107**, 122601 (2015).

[100] P. Merino, C. Groe, A. Roslawska, K. Kuhnke, and K. Kern, *Nature Commun.* **6**, 8461 (2015).

[101] C. Grosse, A. Kabakchiev, T. Lutz, R. Froidevaux, F. Schramm, M. Ruben, M. Etzkorn, K. K. U. Schlickum, and K. Kern, *Nano Lett.* **14**, 5693 (2014).